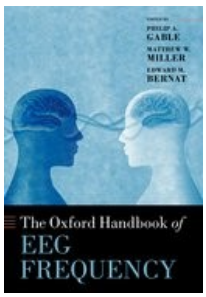

The Oxford Handbook of EEG Frequency

Philip A. Gable (ed.) et al.

https://doi.org/10.1093/oxfordhb/9780192898340.001.0001

Published: 2022 **Online ISBN:** 9780191924729 **Print ISBN:** 9780192898340

CHAPTER

16 Cortical Source Localization in EEG Frequency Analysis

Wanze Xie, John E. Richards

https://doi.org/10.1093/oxfordhb/9780192898340.013.16 Pages 377–C16.P136

Published: 21 September 2022

Abstract

Source localization of EEG signals identifies the loci of neural activity that generates the EEG voltage or power distribution on the scalp. This chapter provides a practical guide to source localization and its usage in EEG analysis in the frequency domain. Techniques proposed to overcome the inverse problem of source localization have progressed from equivalent dipole modeling to distributed source modeling, such as sLORETA and eLORETA. This chapter discusses the rationale behind these techniques, as well as the advantages and disadvantages of using different techniques for source localization. Recent advances in high-resolution structural MRI make it possible to accurately delineate and model the tissues inside the head. This chapter discusses the importance of using realistic head models constructed with anatomical MRIs for EEG source localization. Finally, it reviews the applications of source localization as a neuroimaging tool in EEG frequency analysis.

Keywords: frequency source localization, MRI head model, sLORETA, eLORETA, dipole, distributed source model, inverse solution

Subject: Cognition and Behavioural Neuroscience, Neuroscience

Series: Oxford Handbooks

16.1 Introduction to Source Localization

EEG signals recorded via electrodes placed on the scalp represent the postsynaptic potentials generated by mass synchronized pyramidal neurons perpendicular to the cortical surface. Source localization or source analysis is the activity that aims to identify the underlying cortical generators or sources of the EEG potentials measured on the scalp. The sources of the EEG signals may be modeled as electrical dipoles with both directionality and amplitude. The identification of the location of dipoles is often obscured because the current generated by these sources spreads in all directions in the brain and is smeared by the skull. However, recent advances made in improving the techniques for source localization have substantially increased the spatial resolution of this method and led to the tendency towards using it as a brain imaging tool (Michel & Murray, 2012).

Source localization consists of procedures creating a forward (Hallez et al., 2007) and an inverse (Grech et al., 2008) model. The forward model is created with a head model and electrodes and describes the effect of an electrical source inside the head on the EEG. The inverse model is the "inverse" of the forward model and is used with the EEG recording to compute the location and amplitude of the sources that generated the given EEG. The present chapter provides an overview of some widely adopted source analysis techniques and their applications to EEG frequency analysis. The importance of using realistic head models for source analysis is also discussed. In the last section of the chapter, we present examples for using source analysis as a neuroimaging tool in EEG frequency analysis.

p. 378

16.2 Source Localization Techniques and Solutions to the Inverse Problem

There are two major approaches to source localization. Equivalent current dipole (ECD) models use a limited number of electrical dipoles that are computed with the forward model to explain the distribution of the EEG on the scalp. Distributed source models use a large set of dipole locations distributed across the brain and are calculated using the inverse model and the observed EEG to generate the amplitude of the current density (He et al., 2018; Michel et al., 2004). This section presents both models and describes how these models are used for source analysis.

16.2.1 Equivalent Current Dipole Source Localization

ECD modeling assumes that the electrical potential over the entire scalp can be explained by a small set of source dipoles (He et al., 1987). These hypothetical dipoles can vary in position, magnitude, and orientation in a 3D space. We can estimate the dipole parameters by repeated optimization of the parameters of the model so that the dipoles multiplied by the forward model fit the scalp distribution. Alternatively, a set of a priori fixed locations can be set based on theoretical specifications of the known effects, and thus only the parameters of orientation and magnitude are estimated. The ECD models are overdetermined because the number of dipole parameters is significantly less than the number of surface sensors (i.e., EEG electrodes), as the number of the estimated dipole parameters needs to be smaller than the number of electrodes on the scalp to guarantee a unique (overdetermined) solution (Michel et al., 2004).

A forward model needs to be constructed to estimate the electrical activity over the scalp in ECD modeling, as well as distributed source modeling. The forward model represents the head geometry and tissue conductivity and delineates how the activation generated by the dipoles propagates to the scalp; the so called "lead-field" matrix. The estimated electrical activity over the scalp is calculated by applying the forward model to the current dipoles with certain orientations and magnitudes (i.e., the forward solution). For ECD modeling, the output of this so-called forward solution can be compared to the actual electrical activity on the scalp, and thus the amount of variance explained by the selected current dipoles can be calculated (Richards, 2003; Scherg, 1992). The optimal solution is gained through the iteration of the forward solution with different parameters (location, orientation, and magnitude) of the dipoles until the minimal residual variance is obtained (Scherg et al., 1999).

A practical concern associated with equivalent current dipole modeling is the uncertainty about the number of dipoles and their locations that should be tested by the forward solution. One solution to this concern is to

p. 379

make a priori assumptions of the ↳ number and location of dipoles based on other neuroimaging data, such as functional magnetic resonance imaging (fMRI) and positron emission tomography (PET) (Agam et al., 2011; Foxe et al., 2003). For example, a meta-analysis of previous fMRI reports was conducted by Foxe and colleagues (2003) to find out the brain regions that were consistently activated in the attention task used by

the authors. The location of these regions was used as a guide in their source analysis, such that the MRI coordinates of these areas were used as the seeds for the dipoles in the forward solution, with the assumption that the task-related EEG activity was generated in these areas. A priori assumptions can also be made based on theoretical rationale and findigns from previous research, such as using the fusiform and occipital face area (FFA; OFA) as the potential sources for the N170 component (Gao et al., 2019), the occipital and parietal regions for alpha oscillations (Xie et al., 2017), and the pre-central cortex for the mu rhythm (Thorpe et al., 2016). Gao and colleagues (2019) conducted a thorough literature review of the cortical source locations of the N170 ERP component found by previous EEG studies and the 3D coordinates of the FFA identified by previous fMRI research, and then used these locations as a priori defined regions of interest (ROIs) in their cortical source localization. Section 2.3 provides further information about how to define a priori ROIs for source localization.

16.2.2 Distributed Source Modeling

In distributed source models, cortical dipoles are distributed over the entire source space, and each dipole has a fixed location. The locations of the dipoles are called the "source space". The source space can be GM voxels derived from a structural MRI, the surface of the brain or "inner compartment" in boundary element methods, or the entire brain volume. A forward model is also needed for distributed source modeling. For distributed source modeling, the forward model is combined with the source space to estimate an inverse spatial filter (Grech et al., 2008). The inverse spatial filter, when multiplied by the observed scalp electrical current distribution, reconstructs the current density across the entire set of potential source locations (e.g., the current-density reconstruction [CDR] method).

The computation of the inverse spatial filter is problematic because the inverse of the lead-field matrix is "underdetermined". The relation between the scalp EEG potentials and the source activation can be simplified and illustrated by the following equation with the assumption that this relation is linear: Y (scalp potential) = K·X (source moments) + E (noise). In this equation, K stands for the transfer matrix from brain sources (the electrical "field") to the scalp potentials (the sensor "leads") and is referred to as the lead-field matrix. Mathematically, the source moments can be calculated by a transform of the previous equation: $X = K^{-1} \cdot Y$. Here, K^{-1} is the inverse of the lead-field matrix and referred to as the inverse spatial filter, which can be used to project the measured data on the scalp to the source space. The matrix inversion of K is "underdetermined" because the number of sources is substantially larger than the number of surface
p. 380 electrodes. ↳ Thus, additional constraints must be imposed to obtain unique and well-posed linear inverse solutions (Grech et al., 2008; He et al., 2018).

The solution to the underdetermined construction of the inverse spatial filter is to constrain the solution by mathematical or quantitative procedures (Grech et al., 2008; Michel & He, 2012). The following paragraphs introduce a couple of widely adopted solutions in distributed source modeling: minimum norm estimation (MNE), low-resolution electromagnetic tomography (LORETA), standardized low-resolution electromagnetic tomography (sLORETA), and exact low-resolution electromagnetic tomography (eLORETA). Pascual-Marqui and colleagues have made great contribution to the development of the "LORETA family" in the past two decades (Sherlin, 2009). A number of additional solutions have been developed and utilized by the EEG research community, such as weighted MNE, shrinking LORETA FOCUSS (SLF), local autoregressive average, and beamforming techniques. Detailed description of these methods can be found elsewhere (Grech et al., 2008; Green & McDonald, 2009; Hallez et al., 2007; He et al., 2018).

The first introduced algorithm or constraint to the inverse solution in distributed source modeling was the minimum norm least-squares inverse (Hämäläinen & Ilmoniemi, 1994), often called the MNE. This algorithm minimizes the least-square error of the estimated inverse solution X in the equation described earlier, which means it results in an inverse solution with the lowest overall intensity (Hauk, 2004). The

inverse solution obtained from MNE tends to be biased towards weak and superficial sources (Michel et al., 2004). To overcome the problem of this surface-restricted MNE algorithm, several methods have been developed that keep the basic mathematical relations of the MNE but alter its characteristics to resolve its weaknesses. For example, an early modification was to use a depth-weighting matrix in the formula to account for the MNE's bias toward superficial surfaces.

The LORETA algorithm was devised to add to the MNE by the additional constraint to smooth the sources with a Laplacian filter (Pascual-Marqui et al., 1994). The LORETA method was also designed to solve the "surface source" issue of MNE, such that it favors solutions with strong activation of a large number of sources and punishes solutions with small number of surface sources. The Laplacian of the sources is a measure of spatial roughness. Minimizing the Laplacian of sources leads to lower resolution in the source space, and thus the solution of LORETA algorithm is smoother than MNE and weighted MNE algorithms.

Pascual-Marqui (2002) developed the more widely used inverse algorithm sLORETA, which uses the current density estimate given by the MNE solution and weights the solution by the standardized values of the current density estimate. This partially alleviates the emphasis on superficial sources found in the MNE by enhancing the smaller deeper sources with their lower standard deviation. It was found that sLORETA results in fewer errors in reconstructed sources than MNE (Pascual-Marqui, 2002). The source localization accuracy has been compared using weighted MNE, LORETA, and sLORETA by Monte-Carlo analysis of data with different noise levels and sources with different depth in the brain (Grech et al., 2008). Grech and
p. 381 colleagues found that the sLORETA ↳ algorithm had the lowest level of localization error and fewest ghost sources, which are sources estimated from the inverse solution but not actually present in the simulated data. Therefore, sLORETA outperforms the other methods regarding the accuracy of source localization using simulated data with different levels of artifacts.

The eLORETA algorithm is another member of the "MNE family" that is also built upon the linear weighted MNE inverse solution and has been regarded as improvement over the previously developed LORETA and sLORETA algorithms (Pascual-Marqui, 2007). The eLORETA algorithm provides exact localization with zero error (i.e., no localization bias) to the inverse solution even in the presence of measurement and structured noise in the data. Assuming there is an activated dipole in the brain with an arbitrary orientation and known magnitude, the scalp EEG potentials generated by this dipole can be simulated. Applying the eLORETA algorithm as the inverse solution to the scalp measurement would give reconstructed current density fields. The "zero error localization" property of eLORETA means that there is zero distance between the actual point-test source and the reconstructed source with the absolute maximum amplitude. It should be noted this property has not been achieved by previously published discrete linear distributed source modeling algorithms (Pascual-Marqui, 2007).

Jatoi and colleagues (2014) compared the source localization accuracy between sLORETA and eLORETA for EEG data collected in an experiment with visual stimuli. The eLORETA algorithm was found to have enhanced ability to suppress less-significant sources in the brain compared to sLORETA. Jatoi and colleagues also found that eLORETA gave less localization error and clearer (less blurry) images as compared to sLORETA. As a member of the LORETA family, the moments in neighboring neuronal sources are also highly correlated for eLORETA.

16.2.3 The "Inverse Problem" with EEG Source Analysis

A common criticism of EEG source analysis is the "inverse problem". The complaint is that a unique solution to the underlying dipole sources is not possible, which occurs because an infinite number of dipole distributions can be constructed, combined with the forward model, and produce the same distribution of EEG potentials on the scalp.

The extent to which the inverse problem affects source analysis depends on a number of factors. The ECD modeling is the most problematic type of inverse modeling, as the resulting model can always be improved by adding one more parameter (e.g., another dipole), or a completely different set of dipole parameters (Hallez et al., 2007). There is no perfect solution to the number of dipoles necessary to find a solution with ECD modeling. Some programs using blind optimization techniques result in solutions that are physiologically unsound.

Distributed source modeling partially alleviates the major concerns with the inverse program. Distributed source models require no a priori assumption (nonparametric) of the number of dipoles (sources) in the model. This minimizes the error in source localization due to misspecification of the number and location of
p. 382 the dipoles (Grech et al., ↳ 2008; Michel et al., 2004). For example, using the CDR approach, all potential source locations (e.g., brain volumes) are simultaneously estimated and the relative magnitude of the reconstructed source activity, also called the current source density (CSD), provides the putative locations of the sources. The source space of the distributed source models may be used to constrain the solution to physiologically reasonable positions. For example, since the generation of the EEG occurs in the postsynaptic potentials of the columnar pyramidal cells, the dipoles may be limited to gray matter (GM) and the dipole directions fixed as perpendicular to the cortical surface. These characteristics have led to a growing tendency in the past two decades to replace ECD optimization methods with distributed source modeling.

16.2.4 Applying a priori Information as Constraints to the EEG Inverse Solution

The linear distributed approaches devised to solve the inverse problem estimate all possible source locations simultaneously. However, there are still an infinite number of configurations of source activation that could generate the EEG scalp potentials, unless a specific set of locations are selected in advance. Anatomical and physiological information derived from other imaging modalities like fMRI, PET, and magnetoencephalography (MEG) have been be applied as constraints to the EEG inverse solution (Michel & He, 2012). In these studies, a priori anatomical and psychophysiological information is used as constraints on the inverse modeling in order to obtain a unique solution or reduce the number of potential solutions. The following two paragraphs introduce a few examples.

These external constraints can be imposed on the construction of the forward and inverse models to reduce the inverse solution space a priori (Lei et al., 2011; Phillips et al., 2002a; Phillips et al., 2002b; Yang et al., 2010) or used as a priori defined ROIs in statistical analyses to reduce the family-wise error rate (Gao et al., 2019; Xie et al., 2017). For example, Lei and colleagues (2011) used temporally coherent brain networks derived from fMRI data as the covariance priors of the EEG source reconstruction. This fMRI networks-based source imaging approach outperformed the traditional distributed source localization methods without fMRI priors and efficiently integrated the astonishing temporal resolution of EEG with the high spatial resolution of fMRI. In another study, an fMRI activation map was used as a spatial constraint to the MNE inverse solution, i.e., a fMRI-weighted MNE (Yang et al., 2010). The authors first conducted independent component analysis (ICA) of the EEG time-series. The ICs are then used to construct a regressor to fit in the fMRI signals. The output fMRI activation map was used as a spatial constraint to the estimation of the source distribution underlying its corresponding IC. Reliable source reconstructed time-frequency configuration and functional connectivity maps were obtained by using this method for both simulated and experimental data (Yang et al., 2010).

p. 383 A recent study by Gao and colleagues (2019) investigated the cortical sources of the N170 face-sensitive ERP component. Individual structural MRI, fMRI, and EEG data were collected. The anatomical information of the head and brain was used to create individual realistic head models for source localization. The face-sensitive regions identified during the fMRI scan were used as the a priori defined ROIs in the analyses of

the reconstructed source activity of the N170 component. This procedure reduces the family-wise error rate that would otherwise be caused by multiple comparisons or analyses across all source volumes in the brain.

16.3 Using Realistic Models and Structural MRI for Source Localization

The forward model that is used in both equivalent current dipole models and distributed source models and is created with a head model. The head model in EEG source localization describes media inside the head with their relative electrical conductivity. The head model is the link between the source volumes and the electrical potentials on the scalp in source analysis. The head models for EEG source localization have progressed from spherical models with only two or three compartments to realistic models with all different tissues of the head being segmented and assigned for their own conductivity values. This section introduces the importance of using realistic head models in EEG source analysis and its usage in empirical research. Since this chapter mostly focuses on realistic head models, an overview of other types of head models can be found elsewhere (Grech et al., 2008; Hallez et al., 2007).

16.3.1 The Effect of Distinction between Head Tissues in the Realistic Models for Source Analysis

An accurate head model that describes the materials inside the head and their relative conductivity is beneficial for source analysis (Reynolds & Richards, 2009; Vorwerk et al., 2014). The two most commonly used methods to create a realistic volume conduction head model are the boundary element method (BEM) and finite element method (FEM). The BEM model segments the head into hierarchical compartments with homogeneous conductivity profiles within a compartment. The FEM model defines the conductivity of individual voxels inside the head based on its material. For example, GM, white matter (WM), and cerebrospinal fluid (CSF) would each have its own conductivity value in a FEM model.

p. 384 The creation of the FEM model used to be much more computational demanding than the BEM model (Michel et al., 2004), but the computational efficiency of computers has now been substantially improved, which makes the FEM model more applicable in source analysis. In a recent paper, Vorwerk and colleagues (2018) introduced a MATLAB-based pipeline, the "Fieldtrip-SimBio" pipeline, that aims to reduce the workload for the generation of multicompartment FEM models. This pipeline has been added to the existing package of functions to create FEM models in the Fieldtrip toolbox (Oostenveld et al., 2011), which allows for an easy construction and application of a FEM model for source analysis (Vorwerk et al., 2018).

Many studies have found that it is important to model the inhomogeneous distribution of brain and head tissues (Cho et al., 2015; Vorwerk et al., 2014). Vorwerk and colleagues (2014) comprehensively investigated the influence of modeling versus not modeling certain conductive tissues of the head on the EEG and MEG forward solution. They tested the effect of hierarchically adding new materials to a basic three-compartment head model (brain, skull, scalp) on the accuracy of source localization. Specifically, they tested the effect of the addition of realistic distribution of CSF, GM, and WM, differentiation of the skull spongiosa and compacta, and anisotropic WM conductivities on source localization. The largest increase in the accuracy of signal topography and amplitude from model to model came with the addition of CSF to the three-compartment model, followed by lesser (but still appreciable) increases when adding GM and WM and the anisotropic WM conductivities into the head models. The lack of the GM/WM distinction, or CSF, in the BEM compartment models, would result in considerable errors in the reconstructed source activities, which concurs with Cho and colleagues' (2015) study, which showed that the distinction between these brain tissues in source localization is important for analyzing EEG and MEG functional connectivity between cortical regions. Taken together, these findings highlight the importance of modeling the head conductive compartments as realistically as possible in order to increase the accuracy of source localization.

By contrast, a few other studies have compared the difference between using BEM and FEM models for source localization but found no substantial difference in the reconstructed source activation (Michel & He, 2012). For example, Birot and colleagues (2014) compared the source localization accuracy with LORETA using BEM and FEM models with 38 epileptic patients. These patients underwent scalp EEG and intracranial EEG recordings and subsequent resection surgery. The results of this study implicated that using the BEM and FEM models did not cause a significant difference in the accuracy of source localization (Birot et al., 2014). This finding suggests that the choice of a head model may not be a crucial factor for source localization using distributed localization algorithm for some applications.

16.3.2 The Uncertainty of the Skull-to-Brain Conductivity Ratio in Realistic Head Models

Another important consideration determining the accuracy of the forward and inverse solutions is to
p. 385 correctly model the conductivity of different tissues, especially the ↳ brain-to-skull conductivity ratio (Acar & Makeig, 2013). There is a consensus that the human skull has a much lower conductivity value than the other tissues inside the head. However, there is dispute about the correct skull conductivity value or the skull-to-brain conductivity ratio to use for creating head models (Michel & He, 2012). The ratio of 1/80 is commonly specified as the skull-to-brain conductivity ratio in head models (either spherical or realistic), with their conductivity values being 0.0042 and 0.33 S/m (Siemens per meter, reciprocal of ohm Ω), respectively. The skull-to-brain conductivity ratio of 1/80 originated from studies that measured the electrical properties of brain and head tissues (Gabriel et al., 1996; Rush & Driscoll, 1969). This ratio has been set up as the default in several source localization toolboxes, such as brain electrical source analysis (BESA; Megis Software GmbH, Gräfelfing, Germany) and Fieldtrip (Oostenveld et al., 2011), and widely used in empirical research and simulated studies (Ryynanen et al., 2006).

More recent studies have suggested that the traditional skull to brain conductivity ratio of 1/80 might be misestimated. A few studies have been conducted to estimate or measure the conductivity of human skull, and findings have shown that the correct skull-to-brain conductivity ratio may be between 1/15 to 1/30, which is much higher than the traditional ratio, and using a lower skull-to-brain conductivity ratio (e.g., 1/80) may result in shallower source locations (Acar et al., 2016; Acar & Makeig, 2013; Dannhauer et al., 2011; Lai et al., 2005; Oostendorp et al., 2000). Therefore, the traditional ratio of skull-to-brain conductivity may need to be adjusted when creating head models for cortical source localization.

Bone conductivities are age dependent, with infants and children having much higher skull conductivity values compared to adults (Odabaee et al., 2014). This means that using the adult skull conductivity values to create head models for infant and child participants could lead to inaccurate source localization results (Reynolds & Richards, 2009). To this end, some source localization software, for example, BESA, provides references for the skull-to-brain conductivity ratio for children and adolescents at different ages. Recent studies have also started to adopt age-appropriate skull conductivity values for source localization on infant EEG data (Xie, Jensen, et al., 2019).

16.3.3 The Importance of Realistic Head Models for Source Localization in Pediatric Populations

Using age-specific realistic head models for source analysis may be especially important for pediatric populations. This is because there are substantial neuroanatomical changes of the tissues inside the head over childhood, and the structure of a child brain differs greatly from an adult brain (Phan et al., 2018; Reynolds & Richards, 2009; Richards, W., 2015). For example, skull conductivity value and thickness are age dependent (Wendel, Vaisanen, Seemann, Hyttinen, & Malmivuo, 2010), such that the skull conductivity value is much higher for infants than adults (Odabaee et al., 2014). Using the adult skull conductivity values for infant EEG data may have the effect of inferring the source of the current as being shallower in the cortex than where it actually occurs.

p. 386 A significant advance in cortical source analysis with pediatric participants is to use realistic head models created with individual MRIs or an age-appropriate MRI template (Guy et al., 2016; Hämäläinen et al., 2011; Ortiz-Mantilla et al., 2012; Xie et al., 2017). Although systematic estimation of skull conductivity for infants and children at different ages has not been conducted, studies have tried to use higher skull conductivity values for source localization for infants and young children data (Hämäläinen et al., 2011; Ortiz-Mantilla et al., 2012; Xie et al., 2018). There are now age-specific MRI templates available to the public for research purposes, which can be used to create realistic head models for children (e.g., the Neurodevelopment MRI Database) (Richards et al., 2016). Since the fontanels and unmended skull sutures of an infant head could allow current flow to the scalp unimpeded by the skull, a future direction is to take the fontanels and skull sutures and the conductivity and topographical differences between infants' and adults' heads into account when creating the realistic head models for infants.

16.4 Application of Source Localization in EEG Frequency Analysis

Human brain oscillatory activity is generated by neural tissue in the central nervous system spontaneously or in response to stimuli in the environment. The significance of these oscillatory signals in sensory-cognitive processes has become increasingly evident. Using source localization in EEG (time) frequency analysis has made great contributions to our understanding of the cortical mechanisms of cognitive processes associated with oscillatory activities in various frequency bands. Using source localization of EEG signals to obtain reconstructed cortical activities also allows us to investigate functional connectivity withing and between brain networks during cognitive tasks and resting-state. The current section reviews the application of source localization techniques in EEG frequency analysis and how this method has provided insights into brain functions and network organizations.

16.4.1 EEG Source Localization in Frequency Analysis for Cognitive Functions

The neural generators of brain oscillatory activity in different frequency bands during cognitive tasks are of great interests to the EEG community. The functional significance of cortical oscillations in low and high frequency bands has been specified using source localization techniques for various cognitive processes,
p. 387 such as spatial attention orienting and attentional control (Doesburg et al., 2009; Jones et al., 2010; Sauseng ↳ et al., 2007), sustained attention and vigilance (Kim et al., 2017), error monitoring and conflict processing (Cohen, 2011; Cohen & Ridderinkhof, 2013; Yeung et al., 2007), working memory (Maurer et al., 2015; Michels et al., 2010; Michels et al., 2008; Onton et al., 2005), motion observation and execution (Nystrom et al., 2011; Ritter et al., 2009; Thorpe et al., 2016). There is a large body of literature on the developmental origin of the relation between these cognitive processes and corresponding EEG oscillations (Bell & Cuevas, 2012). EEG source localization has also made it possible to investigate the cortical sources of EEG oscillatory activities associated with cognitive performance in infants and children (see Section 16.4.4).

The source localization techniques discussed in the previous sections open the avenue to unravel the crucial role of EEG oscillatory activity in human brain functions. For instance, Sauseng and colleagues (2007) investigated the function of the theta-band oscillations in sustained attention and executive control. They examined how EEG theta-band activity changed as a function of task difficulty and memory load. The participants were required to execute complex sequential finger movements requiring different levels of memory load, such as execution of a previously trained simple sequence, an overlearned complex sequence, or a novel complex sequence. Local frontal-midline theta activity on the scalp was found to be associated with the general level of cognitive demand, with the highest power found for the most demanding condition. This theta activity was reconstructed to the source space using the LORETA method. Specifically, the CSD was reconstructed for more than 2000 cortical voxels across the brain using distributed source modeling, separately for different cognitive conditions. The source activity was then compared voxel by voxel between the conditions, and multiple comparisons were statistically controlled. The authors found that the CSD in the anterior cingulate gyrus was significantly different between the conditions, suggesting that theta-band oscillations generated by this region may reflect the activation of an attentional system responsible for allocating cognitive resources (Sauseng et al., 2007).

Theta-band activity generated by the frontal cortex also plays an important role in error monitoring (Cohen, 2011). Cohen found that EEG theta-band activity in the frontal electrodes was associated with error-monitoring behaviors in adults. The author subsequently conducted source localization of the theta-band activity using equivalent current dipole modeling with subject-specific BEM models created with individual MRIs. One dipole that explained the most amount of variance of the scalp potentials was estimated per subject. The author found that the dipoles in the medial prefrontal and anterior cingulate cortexes best explained the variance in the frontal theta activity across subjects, suggesting that these areas are the potential sources of the distribution of the theta activity on the scalp.

EEG oscillations generated by the frontal area has been found to play an important role in maintaining vigilance (sustained attention) during cognitive tasks. Kim and colleagues (2017) investigated which brain areas are engaged in controlling the maintenance of vigilance using source analysis of EEG signals. Distributed source modeling with the sLORETA algorithm was conducted to obtain smooth source activation
p. 388 in different frequency bands across the entire cortex. The authors found that the activity in the left ↳ prefrontal cortex was significantly correlated with vigilance variation in the delta, beta, and gamma bands, which suggests the involvement of this brain region in maintaining vigilance. To sum up, these empirical studies demonstrated how using EEG source analysis in frequency analysis could advance our understanding of the neural mechanisms underlying different cognitive processes.

16.4.2 EEG Source Localization for Clinical Applications

Imaging the neuronal activity that generates the scalp EEG oscillations is also desirable for clinical purposes. EEG source imaging offers a useful tool to help presurgical evaluation of patients with epilepsy in a noninvasive way, as identifying the cortical epileptic zone for ictal oscillations is crucial for surgical resection. The decent accuracy (~80%) of using EEG source localization in determining the subsequently resected zone has been consistently achieved across studies on pediatric (Lu et al., 2012) and adult patients (Brodbeck et al., 2011; Yang et al., 2011). For example, Brodbeck and colleagues investigated the sensitivity and specificity of using EEG source imaging to detect the epileptic zone for over 150 patients who underwent surgery later. The authors found that using EEG source imaging resulted in high sensitivity (84%) and specificity (88%) in detecting the seizure zone. The obtained sensitivity and specificity values were even higher than some conventional neuroimaging tools (e.g., fMRI and PET). It should be noted that acceptable localization results were only obtained when a large number of electrodes (>128 channels) were used for data collection (Brodbeck et al., 2011), which suggests the importance of using sufficient electrodes to obtain a better resolution of the topographic features, that is, to avoid distortions of the distribution of scalp potentials due to large distances between electrodes (see Michel et al., 2004 for a thorough review of the effect of the number of electrodes). Spectral analysis of EEG with source localization techniques has also been applied to characterize difficulties in brain functioning for other clinical populations, such as children with ADHD (Liotti et al., 2005), people with tonic pain (Canuet et al., 2012), and Parkinsonian patients (Moazami-Goudarzi et al., 2008).

16.4.3 Applying EEG Source Analysis to Studying Functional Brain Connectivity in the Frequency Domain

One critical question in the field of cognitive neuroscience is how brain regions in large-scale networks communicate and cooperate with each other during tasks and resting-state. The application of neuroimaging tools makes it possible for researchers to investigate the dynamic interregional communications inside the brain and their development throughout the lifespan. Using fMRI allows people to obtain images of the blood-oxygen-level dependent (BOLD) signals in brain voxels. However, the
p. 389 temporal resolution of the BOLD response in fMRI depends on blood flow occurring several ↳ seconds following the demand for glucose via oxygenated hemoglobin. This restricts fMRI connectivity analyses to "seconds" resolution and prohibits this technique from studying dynamic changes in neural oscillations in sub-second frequency ranges. By contrast, EEG and MEG directly measure synchronized neuronal activity with msec time resolution and thus can measure dynamic changes in neural oscillations at the resolution of the neural system (e.g., sub-seconds resolution).

The examination of EEG functional connectivity between electrodes on the scalp has been used to study synchronized fluctuations in various rhythms that may reflect the dynamic coordination and network structure inside the brain (Bastos & Schoffelen, 2016; Stam, 2005). A variety of methods have been developed to evaluate the "correlation or synchronization" between the signals from two electrodes, such as the correlation between power envelope (Hipp et al., 2012), coherence analysis (Bowyer, 2016), and phase synchronization (Stam et al., 2007). In addition, previous work studying EEG functional connectivity on the scalp level with infants and children provides insights into the developmental origin of integrated brain networks (see Chu-Shore et al., 2011 for a review). For example, Cuevas and colleagues (2012) investigated the association between infants' working memory and inhibitory control performance in cognitive tasks and the coherence between frontal electrodes in the alpha band. The authors found that frontal alpha coherence was associated with inhibitory control processes in 10-month-old infants, which suggests that the cooperation between brain regions already plays an important role in cognitive performance in infancy (Cuevas et al., 2012).

The volume conduction/field spread issue of surface EEG and the effect of the reference electrode on phase synchronization and correlation values impede our understanding of the underlying neural mechanisms from the EEG functional connectivity results on the scalp (Bastos & Schoffelen, 2016; Guevara et al., 2005; Schiff, 2005). Specifically, this problem means that the activity of a cortical source can be "visible" at multiple electrodes due to the field smearing on the scalp. This will cause spurious correlation or synchronization values between electrodes. Consequently, the interpretation of the scalp-level connectivity requires considerable caution because two "connected or synchronized" electrodes may not reflect the brain regions that are functionally connected.

Applying cortical source reconstruction methods to EEG data could substantially mitigate the consequence of volume conduction. Brain functional connectivity using EEG could be done by first estimating the sources of the surface signals, deriving time-domain activity of the cortical sources via the time-domain activity of the surface activity, and then doing functional connectivity in the source-space by calculating the correlation between amplitudes (or power envelope) of times-series in cortical sources or phase synchronization in different frequency bands after Fourier transformation of the time-series in cortical sources into the frequency domain. For example, Xie and colleagues (2018) developed a pipeline to estimate functional connectivity in the cortical source space to investigate the function of different brain networks of awake infants (Figure 16.1). This pipeline includes cortical source reconstruction of EEG recordings with
p. 390 age-appropriate MRIs, parcellation of the source activity into brain ROIs, ↳ estimating brain functional connectivity between ROIs by calculating the weighted phase-lag index (wPLI) (Vinck et al., 2011), and applying graph theory measures to examine the overall architecture of brain networks (Figure 16.1). Using this pipeline, the authors studied how functional connectivity in infant brain networks, such as the dorsal and ventral attention, default mode, and somatosensory networks, changes across different attentional
p. 391 states. For instance, they showed that infant sustained attention is ↳ associated with attenuated connectivity in the alpha band within the dorsal attention network and the DMN, as well as distinct network organization and efficiency indicated by graph theory measures (Xie et al., 2018). This work highlights the possibility of using source-space functional connectivity analysis to study the development of brain networks in early childhood. The following paragraphs introduce more recent advances that have been made in combining EEG source localization and functional brain connectivity analysis in the frequency domain.

Figure 16.1

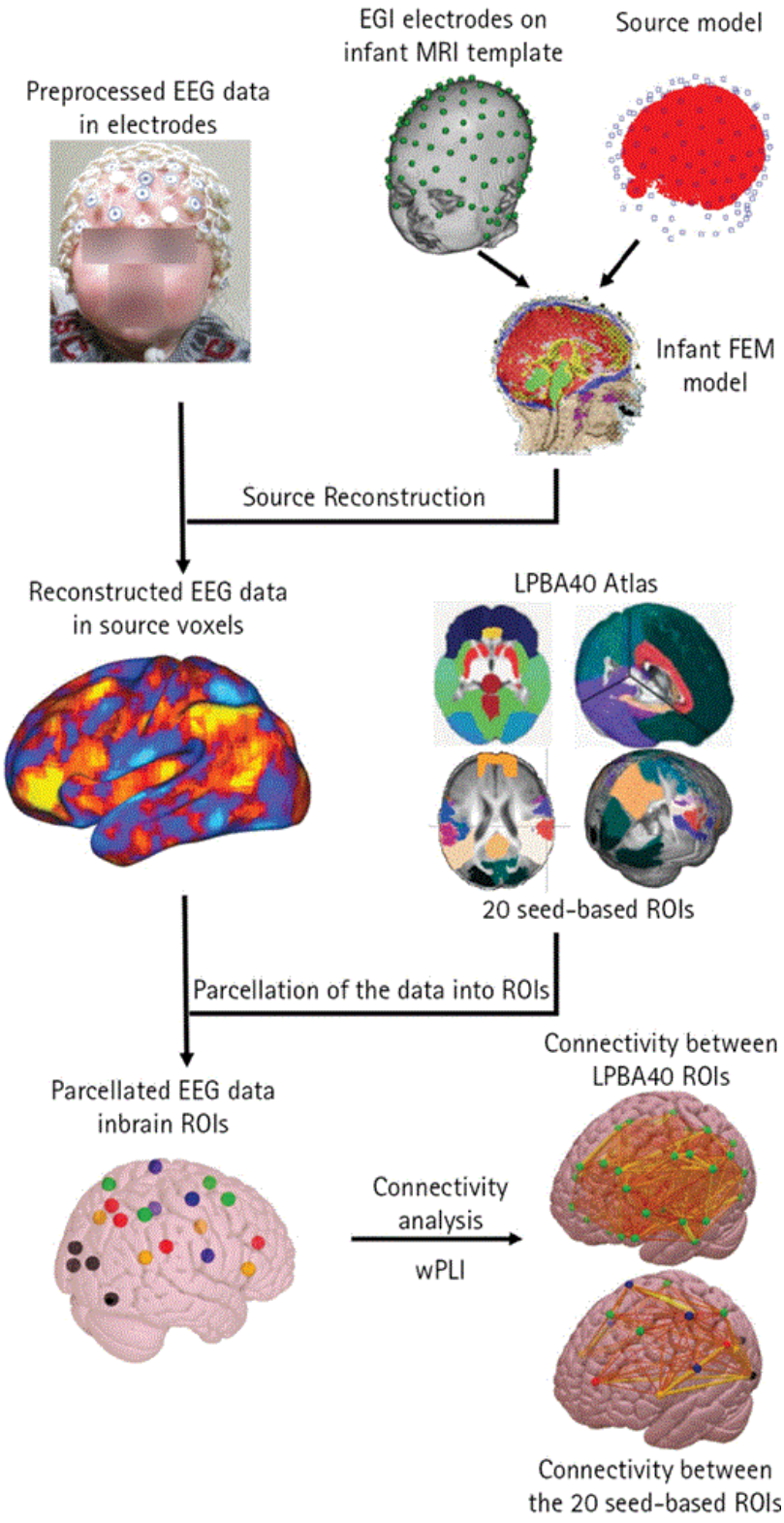

The pipeline for EEG functional connectivity analysis in the source space used by Xie et al. (2018).

EEG source localization can be used to detect brain functional connectivity during tasks. The functional connectivity between frontal and parietal cortices plays an important role in executive control. Sauseng and colleagues (2007) found a more distributed pattern of functional connectivity in the theta band between frontal and parietal regions when participants executed novel compared to memorized figure movement sequences. In a more recent study, Cohen and Ridderinkhof (2013) investigated the functional coupling

between EEG signals in different frequency bands during spatial conflict processing. Inter-regional connectivity in the source space was found to differ between the congruent and incongruent conditions in a Simon task. Congruent trials induced stronger coupling between frontal theta and parietal alpha and gamma power, while incongruent trials induced stronger coupling of the theta power between the medial and lateral frontal regions. Studies also show that the inter-regional phase synchrony in low- and high-frequency bands is associated with top-down control of visual and auditory spatial attention (Doesburg et al., 2009; Doesburg et al., 2012). For example, Doesburg and colleagues (2009) found increased phase synchronization in the alpha band between the visual cortex and parietal regions contralateral to the attended visual hemifield and decreased phase synchronization between those brain regions ipsilateral to the attended visual hemifield. The Cohen and Doesburg studies used the beamforming technique for cortical source reconstruction. The beamforming techniques are not covered here and have been reviewed elsewhere (Green & McDonald, 2009).

The functional connectivity analysis in the source space of spontaneous EEG during resting-state has provided insights into the structure and functioning of brain networks, as well as the development of brain networks over childhood. Liu and colleagues (2017) detected large-scale brain networks in human adults using high-density EEG recordings along with the eLORETA technique and realistic head models for source analysis. ICA analysis of source reconstructed power envelops was conducted to extract functionally connected brain regions (networks) in different frequency bands. Their results showed that the brain networks identified with resting-state EEG data (e.g., the DMN, attention and language networks) were comparable to the brain networks obtained from prior resting-state fMRI research (Liu et al., 2017). Mantini and colleagues' (2007) simultaneous EEG-fMRI data were collected during resting-state to unravel the direct relationship between functional connectivity measured by the two metrics. Six major brain networks (e.g., the DMN, auditory, visual, and attention networks) were identified from the BOLD signals using ICA. The fluctuations in each of these fMRI-defined resting-state networks were found to be correlated with EEG
p. 392 power in different frequency bands ↳ (e.g., delta, theta, alpha, beta, and gamma). This study was one of the first attempts to explore the link between EEG brain rhythms and low-frequency coherent fluctuations of the BOLD signal during resting-state.

16.4.4 EEG Source Localization in Frequency Analysis for Pediatric Populations

High-density EEG offers an easy-to-use tool to measure brain functions for pediatric populations. It is often the method of choice when measuring brain activity in awake infants and older children due to its superb temporal resolution, easy application, low-cost of recordings and relatively higher tolerance to children's movements compared to other neuroimaging tools. Using EEG also makes it possible to monitor infant brain activity corresponding to infant behaviors during cognitive tasks, for example, attention (Xie et al., 2017), emotion processing (Xie et al., 2018) and recognition memory (Reynolds & Richards, 2005) tasks, which could not be done with fMRI. In addition, recent advances made in EEG source localization techniques, as reviewed earlier in the chapter, have made EEG a comprehensive and powerful brain imaging tool with reasonable spatial and superior temporal resolution (Michel & Murray, 2012). Therefore, there is growing interest in using source analysis techniques with high-density EEG recordings to examine the development of the cortical sources of neural oscillations in different frequency bands during childhood. This section gives an overview of recent progress made in using EEG source localization along with frequency analysis as a neuroimaging tool to study brain and cognitive development.

The mu rhythm ("central alpha") has been proposed to be associated with a putative human mirror neuron system (Marshall & Meltzoff, 2011). EEG source localization has been utilized to study the neurodevelopmental origin of the mirror neuron system and the functional significance of the mu rhythm during early childhood. Thorpe and colleagues (2016) investigated the structural development of the mu rhythm during motor execution. The source analysis of the mu rhythm was conducted using the sLORETA

algorithm with age-appropriate head models. The results of this study showed distributed frontoparietal patterns of cortical activation in the mu rhythm. Specifically, the source locations of the mu rhythm were concentrated in the pre- and post-central gyri and the precuneus and inferior parietal regions. The source locations of the mu rhythm were found to be consistent across three age groups—the 1- and 4-year-olds and the adults. The finding of the posterior regions as part of the sources generating the mu rhythm is reminiscent of two previous studies exploring the cortical generators of the infant mu rhythm using ECD models (Nystrom, 2008; Nystrom et al., 2011). The findings of these studies shed light on the neural generators of the mu rhythm in children and its association with motion observation and execution.

Prior studies have suggested that brain rhythms can be manipulated by infant visual sustained attention. However, the cortical generators of attention associated brain rhythmic activity remained unclear. To fill this knowledge gap, a study by Xie and colleagues (2017) explored the complex patterns of EEG oscillations
p. 393 and their cortical ↳ sources observed during infant sustained attention. Specifically, the authors examined whether infant sustained attention, defined with the infant heart-rate attention model (Richards, 2003), was accompanied by distinct EEG rhythmic activities in the theta, alpha and beta bands in attention-related cortical areas. Cortical source reconstruction of EEG power in different frequency bands was conducted using the eLORETA method. Realistic head models were created for each participant using individual MRIs. Infant sustained attention was found to be accompanied by increased theta power in the orbitofrontal and ventral temporal areas and decreased alpha power in brain regions within the default mode network (DMN). The relation between infant sustained attention and EEG power was not found among infants aged 6 and 8 months, but the relation emerged at age 10 months and became well established by age 12 months (Figure 16.2). This study established the a connection between infant sustained attention and cortical oscillatory activity in the theta and alpha bands.

p. 394 **Figure 16.2**

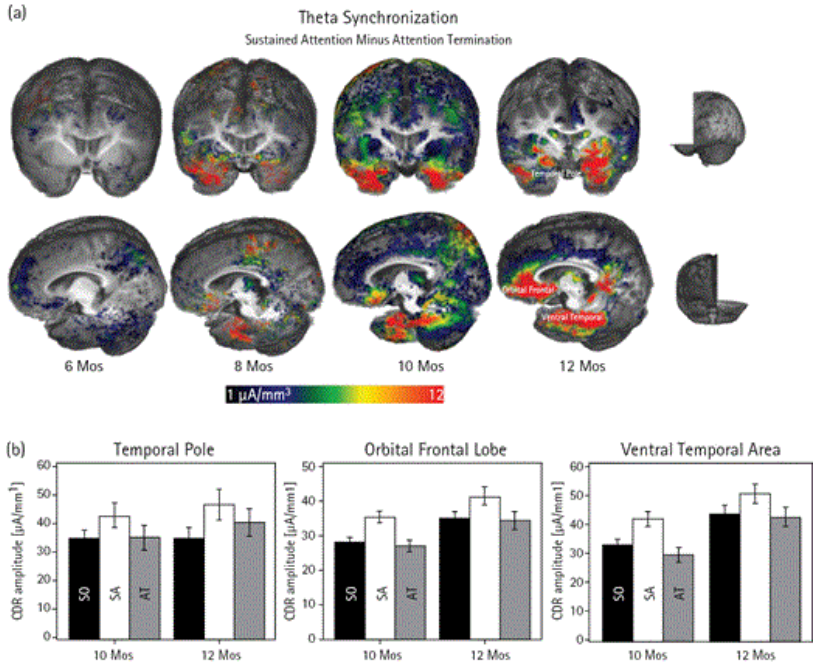

Development of the effect of sustained attention on infant theta source activation. (A) 3D displays for the difference in CDR amplitude between sustained attention and attention termination separately for the four ages. Age-appropriate average MRI templates were used for the display for each age. Sustained attention effect was primarily shown in the temporal pole, orbital frontal, and ventral temporal regions, especially for 10 and 12 months. (B) Bar graphs for the average CDR amplitudes in these brain networks for 10 and 12 months. Error bars represent SEMs.

Adapted from Xie et al., 2017.

Functional connectivity analysis of source reconstructed resting-state EEG signals has recently been adopted to study the development of brain networks with children. Bathelt and colleagues (2013) examined the development of brain network communities using EEG data collected when children between 2 and 6 years of age were in "resting-state" (watching a video clip of calming scenes). Cortical source reconstruction was conducted with age-appropriate head models. Graph theory measures were also employed to assess the organization and efficiency of brain networks. The authors found functional modules that resembled hub networks described for fMRI and developmental changes in graph theory measures (e.g., path length) with age (Bathelt et al., 2013). Similar methods have been used to study how deviations in early experience, such as poverty and growth faltering, shape brain networks in children living in low-income countries (Xie et al., 2019). In a recent study Xie and colleagues explored brain functional connectivity as a mediator of the relation between growth faltering and future cognitive outcomes in a longitudinal sample of impoverished Bangladeshi children. Their results revealed that whole-brain functional connectivity predicted future cognitive function and, perhaps more importantly, that brain functional connectivity at age 36 months mediated the effect of growth faltering on children's IQ assessed one year later.

16.5 Conclusion

This chapter introduces EEG source localization and its usage in (time) frequency analysis. EEG source localization offers superb temporal resolution and increasingly improved spatial resolution. Methodological progress helped to improve the accuracy of source localization, for example, techniques developed to constrain the inverse solutions in distributed source reconstruction. The importance of using realistic head models and age-appropriate conductivity values for source localization is also increasingly recognized by the field, especially for research with pediatric populations. These advances extended the application of source localization in clinical diagnosis and scientific research. Studies using EEG source localization and frequency analysis provide importance insights into the functional significance of oscillatory activities in different frequency rhythms in cognitive processes, as well as the maturation of functional brain networks over development.

References

Acar, A. Z., Acar, C. E., & Makeig, S. (2016). Simultaneous head tissue conductivity and EEG source location estimation. *Neuroimage*, *124*(Pt A), 168–180. doi:10.1016/j.neuroimage.2015.08.032
Google Scholar WorldCat

p. 395 Acar, A. Z., & Makeig, S. (2013). Effects of forward model errors on EEG source localization. *Brain Topography*, *26*(3), 378–396. doi:10.1007/s10548-012-0274-6
Google Scholar WorldCat

Agam, Y., Hamalainen, M. S., Lee, A. K., Dyckman, K. A., Friedman, J. S., Isom, M., … Manoach, D. S. (2011). Multimodal neuroimaging dissociates hemodynamic and electrophysiological correlates of error processing. *Proceedings of the National Academy of Sciences of the United States of America*, *108*(42), 17556–17561. doi:10.1073/pnas.1103475108
Google Scholar WorldCat

Bastos, A. M. & Schoffelen, J. M. (2016). A tutorial review of functional connectivity analysis methods and their interpretational pitfalls. *Frontiers in Systems Neuroscience*, 9, 175. doi:10.3389/fnsys.2015.00175
Google Scholar WorldCat

Bathelt, J., O'Reilly, H., Clayden, J. D., Cross, J. H., & de Haan, M. (2013). Functional brain network organisation of children between 2 and 5 years derived from reconstructed activity of cortical sources of high-density EEG recordings. *Neuroimage*, *82*, 595-604. doi:10.1016/j.neuroimage.2013.06.003
Google Scholar WorldCat

Bell, M. A., & Cuevas, K. (2012). Using EEG to study cognitive development: issues and practices. *Journal of Cognition and Development*, *13*(3), 281–294. doi:10.1080/15248372.2012.691143
Google Scholar WorldCat

Birot, G., Spinelli, L., Vulliemoz, S., Megevand, P., Brunet, D., Seeck, M., & Michel, C. M. (2014). Head model and electrical source imaging: a study of 38 epileptic patients. *Neuroimage: Clinical*, *5*, 77–83. doi:10.1016/j.nicl.2014.06.005
Google Scholar WorldCat

Bowyer, S. M. (2016). Coherence a measure of the brain networks: past and present. *Neuropsychiatric Electrophysiology*, *2*(1), 1. doi:10.1186/s40810-015-0015-7
Google Scholar WorldCat

Brodbeck, V., Spinelli, L., Lascano, A. M., Wissmeier, M., Vargas, M. I., Vulliemoz, S., … Seeck, M. (2011). Electroencephalographic source imaging: a prospective study of 152 operated epileptic patients. *Brain*, *134*(Pt 10), 2887–2897. doi:10.1093/brain/awr243
Google Scholar WorldCat

Cho, J. H., Vorwerk, J., Wolters, C. H., & Knosche, T. R. (2015). Influence of the head model on EEG and MEG source connectivity analyses. *Neuroimage*, *110*, 60–77. doi:10.1016/j.neuroimage.2015.01.043
Google Scholar WorldCat

Chu-Shore, C. J., Kramer, M. A., Bianchi, M. T., Caviness, V. S., & Cash, S. S. (2011). Network analysis: Applications for the developing brain. *Journal of Child Neurology*, *26*(4), 488–500. doi:10.1177/0883073810385345
Google Scholar WorldCat

Cohen, M. X. (2011). Error-related medial frontal theta activity predicts cingulate-related structural connectivity. *Neuroimage*, *55*(3), 1373–1383. doi:10.1016/j.neuroimage.2010.12.072
Google Scholar WorldCat

Cohen, M. X. & Ridderinkhof, K. R. (2013). EEG source reconstruction reveals frontal-parietal dynamics of spatial conflict processing. *PLoS One*, *8*(2), e57293. doi:10.1371/journal.pone.0057293

Google Scholar WorldCat

Cuevas, K., Swingler, M. M., Bell, M. A., Marcovitch, S., & Calkins, S. D. (2012). Measures of frontal functioning and the emergence of inhibitory control processes at 10 months of age. *Developmental and Cognitive Neuroscience*, *2*(2), 235–243. doi:10.1016/j.dcn.2012.01.002
Google Scholar WorldCat

Dannhauer, M., Lanfer, B., Wolters, C. H., & Knosche, T. R. (2011). Modeling of the human skull in EEG source analysis. *Human Brain Mapping*, *32*(9), 1383–1399. doi:10.1002/hbm.21114
Google Scholar WorldCat

Doesburg, S. M., Green, J. J., McDonald, J. J., & Ward, L. M. (2009). From local inhibition to long-range integration: A functional dissociation of alpha-band synchronization across cortical scales in visuospatial attention. *Brain Research*, *1303*, 97–110. doi:10.1016/j.brainres.2009.09.069
Google Scholar WorldCat

Doesburg, S. M., Green, J. J., McDonald, J. J., & Ward, L. M. (2012). Theta modulation of inter-regional gamma synchronization during auditory attention control. *Brain Research*, *1431*, 77–85. doi:10.1016/j.brainres.2011.11.005
Google Scholar WorldCat

p. 396 Foxe, J. J., McCourt, M. E., & Javitt, D. C. (2003). Right hemisphere control of visuospatial attention: Line-bisection judgments evaluated with high-density electrical mapping and source analysis. *Neuroimage*, *19*(3), 710–726.
Google Scholar WorldCat

Gabriel, C., Gabriel, S., & Corthout, E. (1996). The dielectric properties of biological tissues. 1. Literature survey. *Physics in Medicine and Biology*, *41*(11), 2231–2249. doi:10.1088/0031-9155/41/11/001
Google Scholar WorldCat

Gao, C., Conte, S., Richards, J. E., Xie, W., & Hanayik, T. (2019). The neural sources of N170: Understanding timing of activation in face-selective areas. *Psychophysiology*, 56(6), e13336. doi:10.1111/psyp.13336
Google Scholar WorldCat

Grech, R., Cassar, T., Muscat, J., Camilleri, K. P., Fabri, S. G., Zervakis, M., … Vanrumste, B. (2008). Review on solving the inverse problem in EEG source analysis. *Journal of Neuroengineering and Rehabilitation*, *5*, 25. doi:10.1186/1743-0003-5-25
Google Scholar WorldCat

Green, J. J. & McDonald, J. J. (2009). A practical guide to beamformer source reconstruction for EEG. In T. C. Handy (Ed.), *Brain signal analysis: Advances in neuroelectric and neuromagnetic methods* (pp. 76–98). MIT Press
Google Scholar Google Preview WorldCat COPAC

Guevara, R., Velazquez, J. L., Nenadovic, V., Wennberg, R., Senjanovic, G., & Dominguez, L. G. (2005). Phase synchronization measurements using electroencephalographic recordings: what can we really say about neuronal synchrony? *Neuroinformatics*, *3*(4), 301–314. doi:10.1385/NI:3:4:301
Google Scholar WorldCat

Guy, M. W., Zieber, N., & Richards, J. E. (2016). The cortical development of specialized face processing in infancy. *Child Development*, 87(5), 1581–1600. doi:10.1111/cdev.12543
Google Scholar WorldCat

Hallez, H., Vanrumste, B., Grech, R., Muscat, J., De Clercq, W., Vergult, A., … Lemahieu, I. (2007). Review on solving the forward problem in EEG source analysis. *Journal of Neuroengineering and Rehabilitation*, *4*, 46. doi:10.1186/1743-0003-4-46
Google Scholar WorldCat

Hämäläinen, J. A., Ortiz-Mantilla, S., & Benasich, A. A. (2011). Source localization of event-related potentials to pitch change mapped onto age-appropriate MRIs at 6 months of age. *Neuroimage*, *54*(3), 1910–1918. doi:10.1016/j.neuroimage.2010.10.016

Google Scholar WorldCat

Hämäläinen, M. S. & Ilmoniemi, R. J. (1994). Interpreting magnetic fields of the brain: Minimum norm estimates. *Medical & Biological Engineering & Computing*, *32*(1), 35–42.
Google Scholar WorldCat

Hauk, O. (2004). Keep it simple: a case for using classical minimum norm estimation in the analysis of EEG and MEG data. *Neuroimage*, *21*(4), 1612–1621. doi:10.1016/j.neuroimage.2003.12.018
Google Scholar WorldCat

He, B., Musha, T., Okamoto, Y., Homma, S., Nakajima, Y., & Sato, T. (1987). Electric dipole tracing in the brain by means of the boundary element method and its accuracy. *IEEE Transactions on Biomedical Engineering*, *34*(6), 406–414.
Google Scholar WorldCat

He, B., Sohrabpour, A., Brown, E., & Liu, Z. (2018). Electrophysiological source imaging: A noninvasive window to brain dynamics. *Annual Review of Biomedical Engineering*, *20*, 171–196. doi:10.1146/annurev-bioeng-062117-120853
Google Scholar WorldCat

Hipp, J. F., Hawellek, D. J., Corbetta, M., Siegel, M., & Engel, A. K. (2012). Large-scale cortical correlation structure of spontaneous oscillatory activity. *Nature Neuroscience*, *15*(6), 884–890. doi:10.1038/nn.3101
Google Scholar WorldCat

Jatoi, M. A., Kamel, N., Malik, A. S., & Faye, I. (2014). EEG-based brain source localization comparison of sLORETA and eLORETA. *Australasian Physical & Engineering Sciences in Medicine*, *37*(4), 713–721. doi:10.1007/s13246-014-0308-3
Google Scholar WorldCat

Jones, S. R., Kerr, C. E., Wan, Q., Pritchett, D. L., Hamalainen, M., & Moore, C. I. (2010). Cued spatial attention drives functionally
p. 397 relevant modulation of the mu rhythm in ↳ primary somatosensory cortex. *Journal of Neuroscience*, *30*(41), 13760–13765. doi:10.1523/JNEUROSCI.2969-10.2010

Kim, J.-H., Kim, D.-W., & Im, C.-H. (2017). Brain areas responsible for vigilance: An EEG source imaging study. *Brain Topography*, *30*(3), 343–351. doi:10.1007/s10548-016-0540-0
Google Scholar WorldCat

Lai, Y., van Drongelen, W., Ding, L., Hecox, K. E., Towle, V. L., Frim, D. M., & He, B. (2005). Estimation of in vivo human brain-to-skull conductivity ratio from simultaneous extra- and intra-cranial electrical potential recordings. *Clinical Neurophysiology*, *116*(2), 456–465. doi:10.1016/j.clinph.2004.08.017
Google Scholar WorldCat

Lei, X., Xu, P., Luo, C., Zhao, J., Zhou, D., & Yao, D. (2011). fMRI functional networks for EEG source imaging. *Human Brain Mapping*, *32*(7), 1141–1160. doi:10.1002/hbm.21098
Google Scholar WorldCat

Liotti, M., Pliszka, S. R., Perez, R., Kothmann, D., & Woldorff, M. G. (2005). Abnormal brain activity related to performance monitoring and error detection in children with ADHD. *Cortex*, *41*(3), 377–388.
Google Scholar WorldCat

Liu, Q., Farahibozorg, S., Porcaro, C., Wenderoth, N., & Mantini, D. (2017). Detecting large-scale networks in the human brain using high-density electroencephalography. *Human Brain Mapping*, 38(9), 4631–4643. doi:10.1002/hbm.23688
Google Scholar WorldCat

Lu, Y., Yang, L., Worrell, G. A., Brinkmann, B., Nelson, C., & He, B. (2012). Dynamic imaging of seizure activity in pediatric epilepsy patients. *Clinical Neurophysiology*, *123*(11), 2122–2129. doi:10.1016/j.clinph.2012.04.021
Google Scholar WorldCat

Mantini, D., Perrucci, M. G., Del Gratta, C., Romani, G. L., & Corbetta, M. (2007). Electrophysiological signatures of resting state networks in the human brain. *Proceedings of the National Academy of Sciences of the United States of America*, *104*(32), 13170–13175. doi:10.1073/pnas.0700668104
Google Scholar WorldCat

Marshall, P. J., & Meltzoff, A. N. (2011). Neural mirroring systems: exploring the EEG mu rhythm in human infancy. *Dev Cogn Neurosci*, *1*(2), 110–123. https://doi.org/10.1016/j.dcn.2010.09.001
Google Scholar WorldCat

Maurer, U., Brem, S., Liechti, M., Maurizio, S., Michels, L., & Brandeis, D. (2015). Frontal midline theta reflects individual task performance in a working memory task. *Brain Topography*, *28*(1), 127–134. doi:10.1007/s10548-014-0361-y
Google Scholar WorldCat

Michel, C. & He, B. (2012). EEG mapping and source imaging. In D. Schomer & F. H. Lopes da Silva (Eds.), *Niedermeyer's electroencephalography* (pp. 1179–1202). Lippincott Williams & Wilkins.
Google Scholar Google Preview WorldCat COPAC

Michel, C. M., & Murray, M. M. (2012). Towards the utilization of EEG as a brain imaging tool. *Neuroimage*, *61*(2), 371–385. doi:10.1016/j.neuroimage.2011.12.039
Google Scholar WorldCat

Michel, C. M., Murray, M. M., Lantz, G., Gonzalez, S., Spinelli, L., & Grave de Peralta, R. (2004). EEG source imaging. *Clinical Neurophysiology*, *115*(10), 2195–2222. doi:10.1016/j.clinph.2004.06.001
Google Scholar WorldCat

Michels, L., Bucher, K., Luchinger, R., Klaver, P., Martin, E., Jeanmonod, D., & Brandeis, D. (2010). Simultaneous EEG-fMRI during a working memory task: Modulations in low- and high-frequency bands. *PLoS One*, *5*(4), e10298. doi:10.1371/journal.pone.0010298
Google Scholar WorldCat

Michels, L., Moazami-Goudarzi, M., Jeanmonod, D., & Sarnthein, J. (2008). EEG alpha distinguishes between cuneal and precuneal activation in working memory. *Neuroimage*, *40*(3), 1296–1310. doi:10.1016/j.neuroimage.2007.12.048
Google Scholar WorldCat

Moazami-Goudarzi, M., Sarnthein, J., Michels, L., Moukhtieva, R., & Jeanmonod, D. (2008). Enhanced frontal low and high frequency power and synchronization in the resting EEG of parkinsonian patients. *Neuroimage*, *41*(3), 985–997. doi:10.1016/j.neuroimage.2008.03.032
Google Scholar WorldCat

Nystrom, P. (2008). The infant mirror neuron system studied with high density EEG. *Social Neuroscience*, *3*(3-4), 334–347. doi:10.1080/17470910701563665
Google Scholar WorldCat

Nystrom, P., Ljunghammar, T., Rosander, K., & von Hofsten, C. (2011). Using mu rhythm desynchronization to measure mirror neuron activity in infants. *Developmental Science*, *14*(2), 327–335.
Google Scholar WorldCat

Odabaee, M., Tokariev, A., Layeghy, S., Mesbah, M., Colditz, P. B., Ramon, C., & Vanhatalo, S. (2014). Neonatal EEG at scalp is focal and implies high skull conductivity in realistic neonatal head models. *Neuroimage*, *96*, 73–80. doi:10.1016/j.neuroimage.2014.04.007
Google Scholar WorldCat

Onton, J., Delorme, A., & Makeig, S. (2005). Frontal midline EEG dynamics during working memory. *Neuroimage*, *27*(2), 341–356. doi:10.1016/j.neuroimage.2005.04.014
Google Scholar WorldCat

Oostendorp, T. F., Delbeke, J., & Stegeman, D. F. (2000). The conductivity of the human skull: Results of in vivo and in vitro measurements. *IEEE Transactions on Biomedical Engineering*, *47*(11), 1487–1492. doi:10.1109/Tbme.2000.880100
Google Scholar WorldCat

Oostenveld, R., Fries, P., Maris, E., & Schoffelen, J. M. (2011). FieldTrip: Open source software for advanced analysis of MEG, EEG, and invasive electrophysiological data. *Computational Intelligence and Neuroscience*, *2011*, 156869. doi:10.1155/2011/156869
Google Scholar WorldCat

Ortiz-Mantilla, S., Hamalainen, J. A., & Benasich, A. A. (2012). Time course of ERP generators to syllables in infants: A source localization study using age-appropriate brain templates. *Neuroimage*, *59*(4), 3275–3287. doi:10.1016/j.neuroimage.2011.11.048
Google Scholar WorldCat

Pascual-Marqui, R. D. (2002). Standardized low-resolution brain electromagnetic tomography (sLORETA): technical details. *Methods and Findings in Experimental and Clinical Pharmacology*, *24*, 5–12.
Google Scholar WorldCat

Pascual-Marqui, R. D. (2007). Discrete, 3D distributed, linear imaging methods of electric neuronal activity. Part 1: Exact, zero error localization. https://arxiv.org/abs/0710.3341.
WorldCat

Pascual-Marqui, R. D., Michel, C. M., & Lehmann, D. (1994). Low-resolution electromagnetic tomography - A new method for localizing electrical activity in the brain. *International Journal of Psychophysiology*, *18*, 49–65.
Google Scholar WorldCat

Phan, T. V., Smeets, D., Talcott, J. B., & Vandermosten, M. (2018). Processing of structural neuroimaging data in young children: Bridging the gap between current practice and state-of-the-art methods. *Developmental Cognitive Neuroscience*, *33*, 206–223. doi:10.1016/j.dcn.2017.08.009
Google Scholar WorldCat

Phillips, C., Rugg, M. D., & Friston, K. J. (2002a). Anatomically informed basis functions for EEG source localization: Combining functional and anatomical constraints. *Neuroimage*, *16*(3 Pt 1), 678–695.
Google Scholar WorldCat

Phillips, C., Rugg, M. D., & Fristont, K. J. (2002b). Systematic regularization of linear inverse solutions of the EEG source localization problem. *Neuroimage*, *17*(1), 287–301.
Google Scholar WorldCat

Reynolds, G. D. & Richards, J. E. (2005). Familiarization, attention, and recognition memory in infancy: An event-related potential and cortical source localization study. *Developmental Psychology*, *41*(4), 598–615. doi:10.1037/0012-1649.41.4.598
Google Scholar WorldCat

Reynolds, G. D. & Richards, J. E. (2009). Cortical source localization of infant cognition. *Developmental Neuropsychology*, *34*(3), 312–329. doi:10.1080/87565640902801890
Google Scholar WorldCat

Richards, J. E. (2003). Cortical sources of event-related potentials in the prosaccade and antisaccade task. *Psychophysiology*, *40*(6), 878–894.
Google Scholar WorldCat

Richards, J. E., Sanchez, C., Phillips-Meek, M., & Xie, W. (2016). A database of age-appropriate average MRI templates. *Neuroimage*, *124*, 1254–1259. doi:10.1016/j.neuroimage.2015.04.055
Google Scholar WorldCat

Richards, J. E. X. & Xie, W. (2015). Brains for all the ages: Structural neurodevelopment in infants and children from a life-span perspective. In J. Benson (Ed.), *Advances in child development and behavior* (Vol. 48, pp. 1–52). Elsevier.

Google Scholar Google Preview WorldCat COPAC

Ritter, P., Moosmann, M., & Villringer, A. (2009). Rolandic alpha and beta EEG rhythms' strengths are inversely related to fMRI-BOLD signal in primary somatosensory and motor cortex. *Human Brain Mapping*, *30*(4), 1168–1187. doi:10.1002/hbm.20585
Google Scholar WorldCat

Rush, S. & Driscoll, D. A. (1969). EEG electrode sensitivity - an application of reciprocity. *IEEE Transactions on Biomedical Engineering*, *16*(1), 15-&. doi:10.1109/Tbme.1969.4502598
Google Scholar WorldCat

Ryynanen, O. R., Hyttinen, J. A., & Malmivuo, J. A. (2006). Effect of measurement noise and electrode density on the spatial resolution of cortical potential distribution with different resistivity values for the skull. *IEEE Transactions on Biomedical Engineering*, *53*(9), 1851–1858. doi:10.1109/TBME.2006.873744
Google Scholar WorldCat

Sauseng, P., Hoppe, J., Klimesch, W., Gerloff, C., & Hummel, F. C. (2007). Dissociation of sustained attention from central executive functions: local activity and interregional connectivity in the theta range. *European Journal of Neuroscience*, *25*(2), 587–593. doi:10.1111/j.1460-9568.2006.05286.x
Google Scholar WorldCat

Scherg, M. (1992). Functional imaging and localization of electromagnetic brain activity. *Brain Topography*, *5*(2), 103–111.
Google Scholar WorldCat

Scherg, M., Bast, T., & Berg, P. (1999). Multiple source analysis of interictal spikes: goals, requirements, and clinical value. *Journal of Clinical Neurophysiology*, *16*(3), 214–224.
Google Scholar WorldCat

Schiff, S. J. (2005). Dangerous phase. *Neuroinformatics*, *3*(4), 315–318. doi:10.1385/NI:3:4:315
Google Scholar WorldCat

Sherlin, L. (2009). Diagnosing and treating brain function through the use of low resolution electromagnetic tomography (LORETA). In T. Budzynski, H. K. Budzynski, J. Evans, & A. Abarbanel (Eds.), *Introduction to quantitative EEG and neurofeedback: Advanced theory and applications* (2nd ed.), (pp. 83–102). Academic Press.
Google Scholar Google Preview WorldCat COPAC

Stam, C. J. (2005). Nonlinear dynamical analysis of EEG and MEG: Review of an emerging field. *Clinical Neurophysiology*, *116*(10), 2266–2301. doi:10.1016/j.clinph.2005.06.011
Google Scholar WorldCat

Stam, C. J., Nolte, G., & Daffertshofer, A. (2007). Phase lag index: Assessment of functional connectivity from multi channel EEG and MEG with diminished bias from common sources. *Human Brain Mapping*, *28*(11), 1178–1193. doi:10.1002/hbm.20346
Google Scholar WorldCat

Thorpe, S. G., Cannon, E. N., & Fox, N. A. (2016). Spectral and source structural development of mu and alpha rhythms from infancy through adulthood. *Clinical Neurophysiology*, *127*(1), 254–269. doi:10.1016/j.clinph.2015.03.004
Google Scholar WorldCat

Vinck, M., Oostenveld, R., van Wingerden, M., Battaglia, F., & Pennartz, C. M. (2011). An improved index of phase-synchronization for electrophysiological data in the presence of volume-conduction, noise and sample-size bias. *Neuroimage*, *55*(4), 1548–1565. doi:10.1016/j.neuroimage.2011.01.055
Google Scholar WorldCat

Vorwerk, J., Cho, J. H., Rampp, S., Hamer, H., Knosche, T. R., & Wolters, C. H. (2014). A guideline for head volume conductor modeling in EEG and MEG. *Neuroimage*, *100*, 590–607. doi:10.1016/j.neuroimage.2014.06.040
Google Scholar WorldCat

Vorwerk, J., Oostenveld, R., Piastra, M. C., Magyari, L., & Wolters, C. H. (2018). The FieldTrip-SimBio pipeline for EEG forward solutions. *Biomedical Engineering Online*, *17*, 37. doi:10.1186/s12938-018-0463-y
Google Scholar WorldCat

Wendel, K., Vaisanen, J., Seemann, G., Hyttinen, J., & Malmivuo, J. (2010). The influence of age and skull conductivity on surface and subdermal bipolar EEG leads. *Computational Intelligence and Neuroscience*, *2010*, 397272. doi:10.1155/2010/397272
Google Scholar WorldCat

p. 400

Xie, W., Jensen, K. G., Wade, M., Kumar, S., Westerlund, A., Kakon, S. H., … Nelson, C. A. (2019). Child growth predicts brain functional connectivity and future cognitive outcomes in urban Bangladeshi children exposed to early adversities. *BMC Medicine*, *17*, art. no. 199. https://doi.org/10.1186/s12916-019-1431-5
Google Scholar WorldCat

Xie, W., Mallin, B. M., & Richards, J. E. (2017). Development of infant sustained attention and its relation to EEG oscillations: An EEG and cortical source analysis study. *Developmental Science*, *21*, e12562. doi:10.1111/desc.12562
Google Scholar WorldCat

Xie, W., Mallin, B. M., & Richards, J. E. (2018). Development of brain functional connectivity and its relation to infant sustained attention in the first year of life. *Developmental Science*, *22*, e12703. doi:10.1111/desc.12703
Google Scholar WorldCat

Xie, W., McCormick, S. A., Westerlund, A., Bowman, L. C., & Nelson, C. A. (2018). Neural correlates of facial emotion processing in infancy. *Developmental Science*, *22*, e12758. doi:10.1111/desc.12758
Google Scholar WorldCat

Xie, W., Jensen, S. K. G., Wade, M., Kumar, S., Westerlund, A., Kakon, S. H., Haque, R., Petri, W. A., & Nelson, C. A. (2019). Growth faltering is associated with altered brain functional connectivity and cognitive outcomes in urban Bangladeshi children exposed to early adversity. *BMC Med*, *17*(1), 199. https://doi.org/10.1186/s12916-019-1431-5
Google Scholar WorldCat

Yang, L., Liu, Z., & He, B. (2010). EEG-fMRI reciprocal functional neuroimaging. *Clinical Neurophysiology*, *121*(8), 1240–1250. doi:10.1016/j.clinph.2010.02.153
Google Scholar WorldCat

Yang, L., Wilke, C., Brinkmann, B., Worrell, G. A., & He, B. (2011). Dynamic imaging of ictal oscillations using non-invasive high-resolution EEG. *Neuroimage*, *56*(4), 1908–1917. doi:10.1016/j.neuroimage.2011.03.043
Google Scholar WorldCat

Yeung, N., Bogacz, R., Holroyd, C. B., Nieuwenhuis, S., & Cohen, J. D. (2007). Theta phase resetting and the error-related negativity. *Psychophysiology*, *44*(1), 39–49. doi:10.1111/j.1469-8986.2006.00482.x
Google Scholar WorldCat